Applied Catalysis B: Environmental 223 (2018) 60–66

Contents lists available at ScienceDirect

Applied Catalysis B: Environmental

journal homepage: www.elsevier.com/locate/apcatb

The potential of manganese nitride based materials as nitrogen transfer reagents for nitrogen chemical looping

Said Laassiri[a], Constantinos D. Zeinalipour-Yazdi[b], C. Richard A. Catlow[b], Justin S.J. Hargreaves[a,*]

[a] WestCHEM, School of Chemistry, University of Glasgow, Glasgow, G12 8QQ, UK
[b] Kathleen Lonsdale Materials Chemistry, Department of Chemistry, University College London, 20 Gordon Street, London, WC1H 0AJ, UK

ARTICLE INFO

Article history:
Received 13 December 2016
Received in revised form 21 April 2017
Accepted 26 April 2017
Available online 27 April 2017

Keywords:
Manganese nitride
Ammonia production
Nitrogen mobility
Chemical looping

ABSTRACT

A systematic study was carried out to investigate the potential of manganese nitride related materials for ammonia production. A-Mn-N (A = Fe, Co, K, Li) materials were synthesised by nitriding their oxide counterparts at low temperature using $NaNH_2$ as a source of reactive nitrogen. The reactivity of lattice nitrogen was assessed using ammonia synthesis as a model reaction. In the case of Mn_3N_2, limited reactivity was observed and only 3.1% of the available lattice nitrogen was found to be reactive towards hydrogen to yield ammonia while most of the lattice nitrogen was lost as N_2. However, the presence of a co-metal played a key role in shaping the nitrogen transfer properties of manganese nitride and impacted strongly upon its reactivity. In particular, doping manganese nitride with low levels of lithium resulted in enhanced reactivity at low temperature. In the case of the Li-Mn-N system, the fraction of ammonia formed at 400 °C corresponded to the reaction of 15% of the total available lattice nitrogen towards hydrogen. Li-Mn-N presented high thermochemical stability after reduction with hydrogen which limited the regeneration step using N_2 from the gas phase. However, the results presented herein demonstrate the Li-Mn-N system to be worthy of further attention.

1. Introduction

The production of the vast majority of nitrogen containing organic products requires the use of nitrogen building blocks such as HCN, HNO_3 or NH_3 as a source of reactive nitrogen. (*e.g.* aniline synthesis [1,2], Paal-Knorr pyrrole synthesis [3,4]). During the last century, major breakthroughs in reactive nitrogen production have been achieved through the development of several industrial processes: the Haber-Bosch Process [5], the Andrussow Process [6] and the Ostwald Process [7]. However, producing reactive nitrogen is highly demanding in energy and requires the construction of centralized, capital intensive plants. The Haber-Bosch Process, the industrial process for ammonia generation from H_2 and N_2, is probably the most explicit example. Due to the low equilibrium conversion at ambient pressure, the process is conducted under intensive energy consuming conditions (temperature ca. 400–500 °C and pressure ca.150–200 atm) to ensure acceptable process rates [8]. Even in such extreme conditions, dinitrogen and dihydrogen conversion is only partial and un-reacted gases need to be re-circulated. Moreover, the process requires the use of highly purified reactant to avoid catalyst deactivation which adds greater complexity. Considering the environmental and energetic costs of nitrogen fixation reactions, developing more sustainable and economical routes which could be applied in more local context is of critical interest.

In this context, the development of nitrogen transfer reactions from metal nitrides to generate "on demand" in-situ reactive nitrogen under mild conditions constitutes a tantalizing alternative. This approach is based on the mobility of lattice nitrogen and its possible transfer through mechanisms analogous to the Mars-van Krevelen one. Lattice nitrogen reactivity is precedented and studies on nitrogen reactivity of binary nitride metals and their reduction using dihydrogen to yield ammonia at ambient pressure are established in the literature [9,10]. Ternary cobalt molybdenum nitride was also reported for its high nitrogen mobility and its ability to be reduced from Co_3Mo_3N to Co_6Mo_6N under a H_2 atmosphere to generate ammonia at ambient pressure [11]. Related to this concept, Mg_3N_2 has been studied as source of in-situ reactive nitrogen in order to circumvent the use of an external supply of ammonia for the Paal-Knorr pyrrole reaction [12,13]. The ability of some metals

* Corresponding author.
E-mail address: Justin.Hargreaves@glasgow.ac.uk (J.S.J. Hargreaves).

http://dx.doi.org/10.1016/j.apcatb.2017.04.073

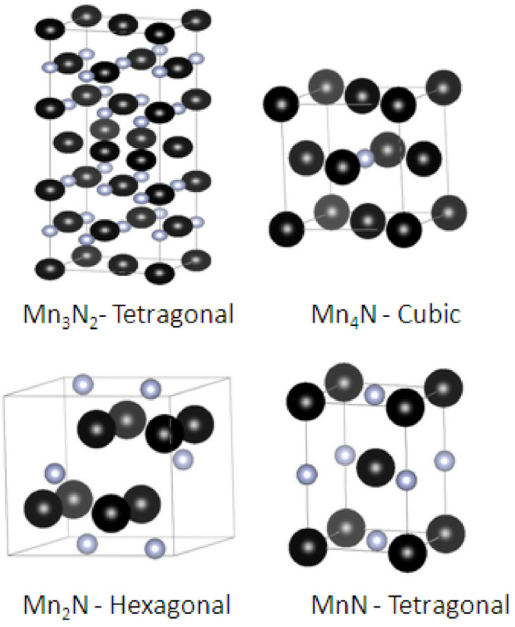

Fig. 1. Manganese nitride structures adapted from reference [22].

to accommodate nitrogen in their structure that could afterwards be available for reaction is of interest for diverse processes including catalytic [14], photocatalytic [15–17] and electrocatalytic [18] ammonia synthesis, particularly if that lattice N can derived from an N_2 source.

Nitrogen chemical looping using nitride materials as nitrogen transfer reagents is an attractive approach to develop combined nitrogen activation in a decentralized manner. In this approach lattice nitrogen can be discharged upon reaction and recharged in a second separated step under different reaction conditions which could alleviate thermodynamic limitations. In such a scheme lattice nitrogen mobility and reactivity under mild conditions are decisive factors for the appropriate choice of the looping material. In recent work, tantalum nitride has been reported as a highly active nitrogen transfer reagent when doped with cobalt. 52% of the total available lattice nitrogen was found to be reactive to hydrogen at ambient pressure to yield ammonia. Post reaction elemental analysis confirmed the reduction of N- content in this material from 8.54 wt.% to 3.04 wt.%. Thus, almost 80% of N- lost during the reaction reacted with H_2 to produce ammonia [19]. Manganese nitride was studied for solar ammonia production where the metal nitride is obtained by dinitrogen reduction at high temperature and subsequently hydrolysed to yield ammonia [20]. The ability of manganese to activate N_2 under ambient pressure to form a range of manganese nitrides [21,22] as presented in Fig. 1 is of relevant interest for the possible development to nitrogen chemical looping reactions. Although manganese nitride is better described as a regenerable reagent in this context, very recent work has reported manganese nitride to be a highly active catalyst for ammonia synthesis at 350 °C when LiH is added as a co-catalyst [23]. However, to date, there is little data relating to the reactivity of the lattice nitrogen in manganese nitride based materials available and the present study aims to address this issue.

Direct reduction using H_2 to yield ammonia has been targeted and the role of dopant metals assessed. The results presented are therefore of interest in both context of development of manganese nitride based N- chemical looping as well as ammonia synthesis catalysed by manganese nitride based systems.

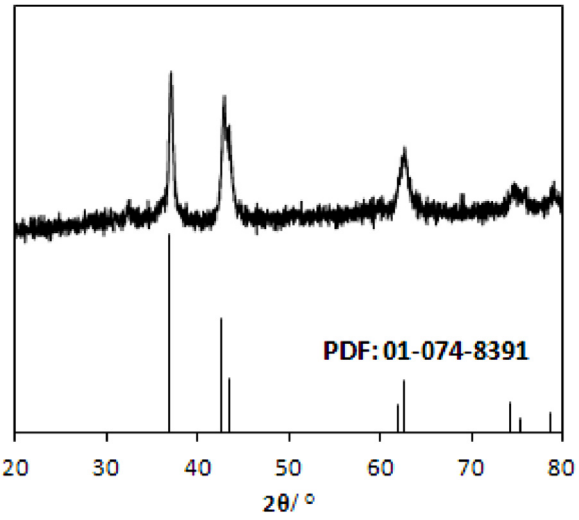

Fig. 2. XRD patterns collected after the nitridation of Mn_2O_3.

2. Experimental section

2.1. Materials synthesis

2.1.1. Preparation of Mn_3N_2

Manganese nitride was prepared using a $NaNH_2$ molten salt synthesis procedure as described in reference [24]. In a typical reaction 0.3 g of Mn_2O_3 (Sigma Aldrich, 99%) and 1.0 g of $NaNH_2$ (Sigma Aldrich, 98%) were loaded into a Teflon-lined steel autoclave inside a nitrogen-filled glovebox. The autoclave was tightly closed and kept in an oven at 240 °C for 36 h. The product was then collected by filtration, and washed with ethanol and water, and dried overnight at room temperature.

2.1.2. Preparation of A-Mn-N materials (A = Li, K, Fe and Co)

A-Mn-O, A = Li, K, Fe and Co systems, with A/Mn molar ratios equal to 1, were prepared by a conventional co-precipitation route, using ammonia as precipitation agent, followed by calcination under static air at 800 °C for 8 h [25]. The nitride phase was then prepared in a similar manner to Mn_3N_2.

2.2. Physical and textural characterisation

2.2.1. Elemental analysis

Nitrogen analysis was undertaken by combustion using an Exeter Analytical CE-440 Elemental Analyser. Error calculations have been performed statistically by repeating the measurement at least twice.

2.2.2. X-ray diffraction

Diffraction patterns were collected on a Siemens D5000 instrument, using CuKα radiation (λ = 0.154 nm) as X-ray source. Recording was performed for between 10° and 80° 2θ (step time = 1 s; step size = 0.02°). Samples were prepared by compaction into Si sample holders. Phase identification is obtained by comparison with JCPDS database files.

2.2.3. Surface area measurement

Surface areas were determined from N_2 physisorption measurements at −196 °C upon samples previously degassed at 120 °C under vacuum for 12 h. The specific surface areas, S_{BET}, were calculated by applying the Brunauer-Emmett-Teller equation.

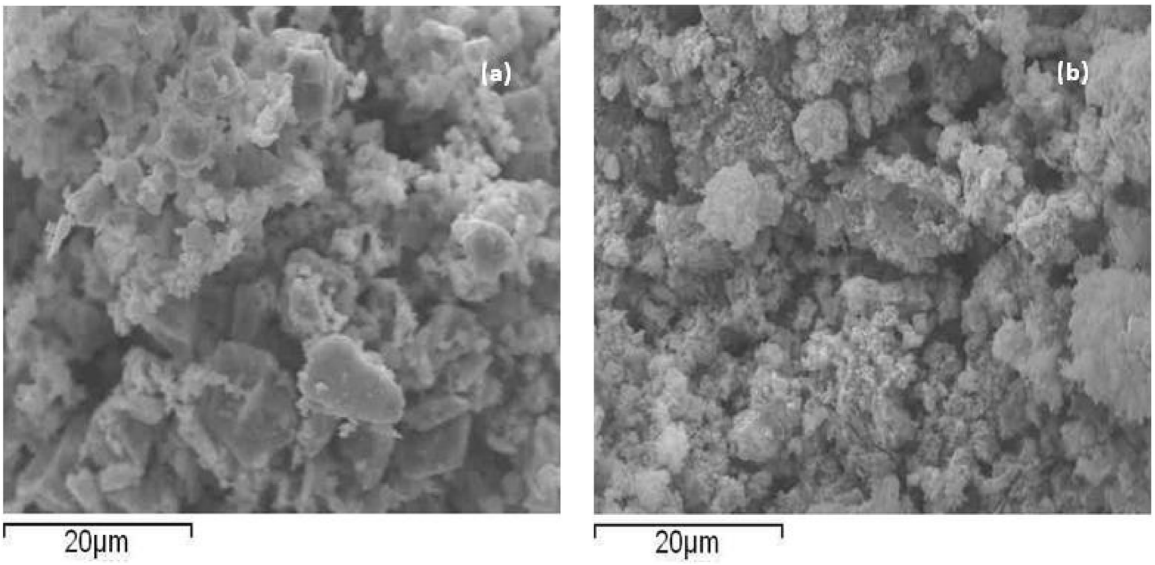

Fig. 3. SEM micrographs of (a) Mn_2O_3, (b) Mn_3N_2.

2.2.4. Scanning electron microscopy

Scanning electron microscopy was performed on Philips XLSE-Mand FEI Quanta 200F Environmental instruments operating at 20 kV. Samples were coated using Au/Pd alloy before SEM imaging.

2.3. Nitrogen transfer properties

The nitrogen transfer properties of manganese based materials were evaluated using ammonia synthesis as a model reaction.

In a typical reaction test, 0.3 g of nitride was placed in the reactor and was pre-treated for 2 h at 400 °C under a 75 vol.% H_2 in N_2 (BOC, 99.98%) gas mixture. The reaction was then performed under a flow composed either of 75 vol.% H_2 in N_2 or 75 vol.% H_2 in Ar (BOC, 99.98%) at a total gas feed of 60 NTP ml min^{-1}. Ammonia production was determined by measurement of the decrease in conductivity of a 200 ml 0.0018 M H_2SO_4 solution through which the reactor effluent stream flowed. The NH_3 yield is reported as the molar ratio of NH_3 generated after a given time (t) relative to the total lattice nitrogen. A schematic of the reactor set up is presented in the supplementary information

Furthermore, ammonia production was confirmed using potassium tetraiodomercurate (Nessler's reagent, Sigma Aldrich) for selected reactions. Error propagation analyses have been performed and are reported for each experiment.

3. Results and discussion

3.1. Structural and textural properties of manganese nitride based materials

XRD patterns and SEM images of the various materials investigated are presented in Figs. 2–6 and Table 1 summarises the structural and textural properties of the prepared nitrides.

3.1.1. Preparation of Mn_3N_2

The XRD pattern recorded after the reaction of Mn_2O_3 with $NaNH_2$ at 240 °C is presented in Fig. 2. All detected reflections matched the tetragonal Mn_3N_2 (PDF number: 01-074-8391). Moreover, the nitrogen content evaluated by elemental analysis was 14.99% wt which is close to that expected based upon stoichiometry (14.53 wt%). From SEM observations, a significant modification in the morphology was observed upon nitridation (Fig. 3). Whilst large

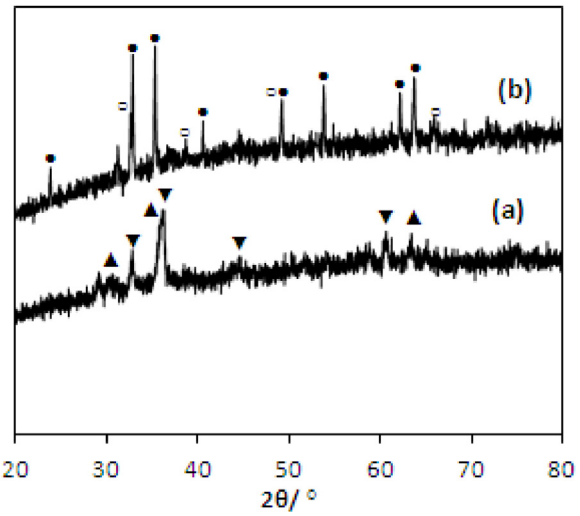

Fig. 4. XRD patterns collected after calcination of (a) Co-Mn-O: ▲ $CoMn_2O_4$ (PDF number: 00-055-068) ▼ Co_2MnO_4 (PDF number: 00-023-1237), (b) Mn-Fe-O: ● Fe_2O_3 (PDF number: 01-085-0987) ○ Mn_2O_3 (PDF number: 01-078-0390).

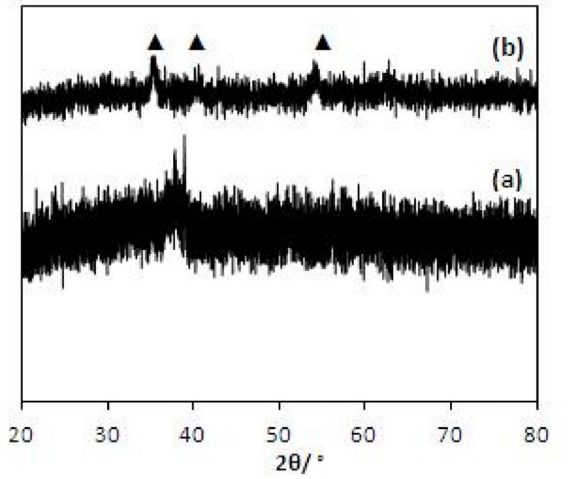

Fig. 5. XRD patterns collected after the nitridation step of: (a) Co-Mn-O, (b) Mn-Fe-O. ▲ Fe_2O_3 (PDF number: 00-002-1165).

Table 1
Physicochemical properties of the prepared materials.

	S_{BET}[a] / $m^2\ g^{-1}$	Phase composition/XRD	Chemical composition	
			N[b]/wt%	A/Mn[c] / molar ratio
Mn_3N_2	66	Mn_3N_2 (PDF number: 01-074-8391)	14.9 ± 0.1	–
Fe-Mn-N	36	Amorphous	10.8 ± 0.1	0.90 ± 0.03
Co-Mn-N	39	Amorphous	13.4 ± 0.2	0.80 ± 0.02
K-Mn-N	10	Mn_3N_2 (PDF number: 01-074-8391)	16.9 ± 0.1	n.d.
Li-Mn-N	11	Mn_3N_2 (PDF number: 01-074-8391)	12.1 ± 0.2	0.10 ± 0.01

n.d. means not detected.
[a] S_{BET} is the specific surface area evaluated using the BET model.
[b] nitrogen analysis undertaken using an Exeter Analytical CE-440 Elemental Analyser.
[c] as evaluated by EDX.

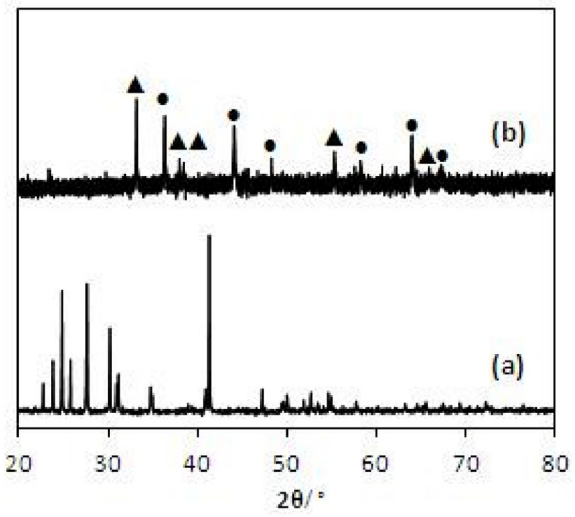

Fig. 6. XRD patterns collected after the calcination step of: (a) K-Mn-O, (b) Li-Mn-O: (▲) LiO2 (PDF number: 01-073-7127), (●) LiMn2O4 (PDF number: 00-018-0736).

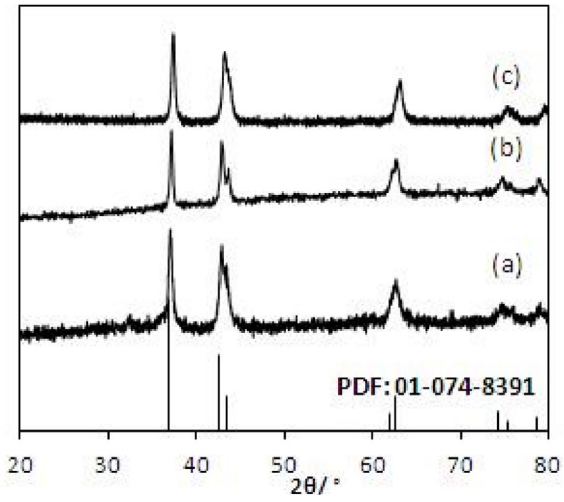

Fig. 7. XRD patterns collected after the nitridation step. (a) Mn_3N_2, (b) K-Mn-N, (c) Li-Mn-N.

micrometric crystals are observed by SEM for Mn_2O_3, large aggregates of smaller Mn_3N_2 were apparent. It is worth mentioning that all attempts to nitride Mn_2O_3 by ammonolysis were unsuccessful and Mn_2O_3 reduction at high temperature resulted in MnO (Fig. S.3).

3.1.2. Preparation of A-Mn-N (A = Fe, Co) materials

Fe-Mn-O and Co-Mn-O oxides were prepared, as precursors for nitridation, by a conventional co-precipitation method followed by calcination at 800 °C for 8 h. XRD patterns of these oxide precursors are presented in Fig. 4. Tetragonal cobalt manganese spinel $CoMn_2O_4$ (PDF number: 00-055-068) was identified along with Co_2MnO_4 (PDF number: 00-023-1237) as the predominant phases in the Co-Mn-O system. No extra-phases related to simple manganese or cobalt oxides were observed (Fig. 4-a). In contrast, only Fe_2O_3 (PDF number: 01-085-0987) and Mn_2O_3 (PDF number: 01-078-0390) were observed in the Fe-Mn-O system and no spinel formation was evidenced by XRD (Fig. 4-b).

Upon nitridation, significant textural and structural modifications were observed in both systems. Surprisingly, the nitridation of Co-Mn-O and Fe-Mn-O resulted in X-ray amorphous materials (Fig. 5-a and -b). Only weak XRD reflections related to Fe_2O_3 (PDF number: 00-002-1165) were observed in the Fe-Mn-O system which may be related to the presence of un-reacted Fe_2O_3. Nevertheless, the strong fluorescence of iron and cobalt induced by the use of copper radiation may strongly influence the XRD line and background intensities thereby hindering phase identification. The nitrogen content of the nitrides was evaluated by elemental analysis. When compared to Mn_3N_2, Fe-Mn-N and Co-Mn-N presented lower nitrogen concentration (10.8 ± 0.1 wt% for Fe-Mn-N and 13.4 ± 0.2 wt% for Co-Mn-N.) Also a significant decrease of the surface area was observed upon second metal addition (66 $m^2\ g^{-1}$ for Mn_3N_2, 36 $m^2\ g^{-1}$ for Fe-Mn-N and 39 $m^2\ g^{-1}$ for Co-Mn-N).

3.1.3. Preparation of A-Mn-N (A = Li, K) materials

In a similar manner to above, A-Mn-N (A = Li, K) materials were prepared using the oxide counterparts as precursors for nitridation. XRD patterns recorded for the oxide are presented in Fig. 6. For K-Mn-O, all reflections relate to $KMnO_4$ (PDF number 00-001-0725) while the Li-Mn-O system was identified to comprise a mixture of $LiMn_2O_4$ (PDF number: 00-018-0736) and of LiO_2 (PDF number: 01-073-7127) However, after the nitridation step only the tetragonal Mn_3N_2 (PDF number: 01-074-8391) was apparent, and no characteristic reflections related to other transition metal nitride or oxide phases were detected (Fig. 7). A small shift towards higher angle is observed for the Li-Mn-N system, when compared to Mn_3N_2, indicating a possible change of lattice parameters. Most of the lithium was found to be lost during nitridation reaction. However, post-nitridation analysis confirmed the presence of lithium in the final products (Mn to Li molar ratio of about 1:10). The effect of alkali metal addition was more apparent upon the textural properties. A significant decrease of the surface areas of the A-Mn-N materials was observed upon alkali metal addition and an effect upon the nitrogen content was also observed (Table 1.) When compared to Mn_3N_2, the Li-Mn-N system showed lower nitrogen content (12.1 ± 0.2 wt%) while a slightly higher content of nitrogen was measured for K-Mn-N (16.9 ± 0.1 wt%).

Table 2
Summary of nitrogen reactivity of manganese nitride based materials after reaction with 60 ml min^{-1} of 1:3 N_2: H_2 at 400 °C.

	Nitrogen content/wt.%		Total N content/μmol/g of material	NH_3 produced/μmol	% lattice N converted to NH_3
	Pre- reaction	Post- reaction			
Mn_3N_2	14.9 ± 0.1	3.45 ± 0.1	10700 ± 11	256 ± 9	3.1
Fe-Mn-N	10.9 ± 0.1	0.1 ± 0.1	7780 ± 8	138 ± 5	1.8
Co-Mn-N	13.4 ± 0.2	1.4 ± 0.1	9565 ± 19	273 ± 9	3.2
K-Mn-N	16.9 ± 0.1	nil	12063 ± 12	73 ± 3	0.2
Li-Mn-N	12.1 ± 0.2	0.5 ± 0.1	8644 ± 17	1306 ± 44	15.8

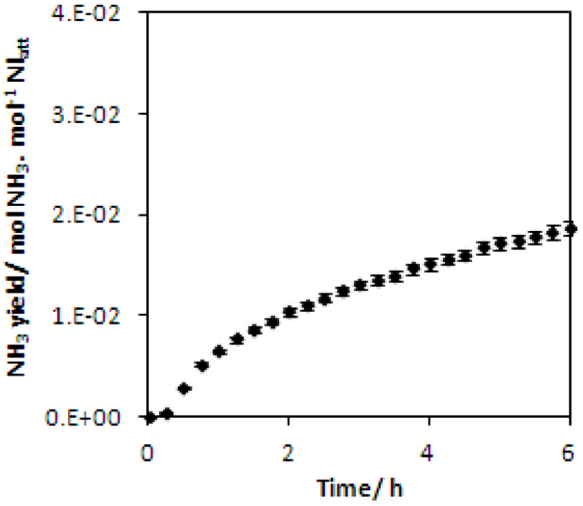

Fig. 8. Ammonia yield of Mn_3N_2 with 60 ml min^{-1} of 1:3 N_2: H_2 at 400 °C. Error propagation within a 95% confidence interval.

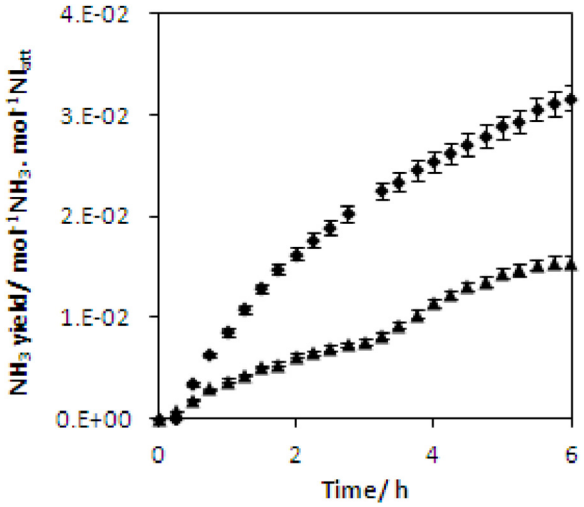

Fig. 9. Ammonia yield of A-Mn-N with 60 ml min^{-1} of 1:3 N_2: H_2 at 400 °C: (▲) Fe-Mn-N, (♦) Co-Mn-N. Error propagation within a 95% confidence interval.

3.2. Reactivity of Mn_3N_2 related system for ammonia generation

3.2.1. Reactivity of Mn_3N_2

The reactivity of Mn_3N_2 lattice nitrogen was investigated using ammonia synthesis as a model reaction using a 60 ml min^{-1} of 3:1 H_2:N_2 (BOC, H_2 99.998%, N_2 99.995%). Ammonia production as function of time at 400 °C is presented in Fig. 8. Over 6 h of reaction, a very limited amount of ammonia, ca 256 μmol. NH_3/g of material, was produced which corresponded to the reaction of 3.1% of the available lattice nitrogen to dihydrogen (Table 2). Post-reaction analysis revealed that 76% of lattice nitrogen was liberated after 6 h of reaction. However, only 3.1% of the lattice nitrogen was reactive towards H_2 to yield NH_3, suggesting that ca. 73% was lost as N_2. Nevertheless, the loss of the vast majority of the lattice nitrogen of Mn_3N_2 at 400 °C contrasts with the thermochemical stability of Mn_4N and $Mn_6N_{2.85}$ reported elsewhere [20]. Differences in crystalline structure and textural and structural properties prepared by different synthesis methods could affect the nitrogen reactivity. The decrease in the lattice nitrogen during the ammonia synthesis reaction confirms the ability of Mn_3N_2 to act as a nitrogen transfer material, although it is not a true catalyst, but rather a reactant in this context, since as reported later in this manuscript, measurements conducted under 1:3 Ar:H_2 presented very similar results.

3.2.2. Reactivity of A-Mn-N (A = Fe, Co)

To study the effect of transition metal in Mn_3N_2 lattice nitrogen reactivity, A-Mn-N, (A = Fe, Co) systems were prepared and tested for ammonia synthesis (Table 2, Fig. 9). Upon iron addition, ammonia synthesis was inhibited and only a very limited amount was produced ca. 138 μmol NH_3/g over 6 h. However, post-reaction elemental analysis showed a considerable reduction of nitrogen content to 0.1 wt%. The amount of ammonia generated corresponded to the consumption of 1.8% of available lattice nitrogen which suggests that iron accelerated lattice nitrogen depletion as N_2 rather than the reaction with H_2. Elsewhere in the literature, the presence of Fe has been reported to destabilise the Mn-N bond in $Mn_6N_{2.58}$ and Mn_4N enhancing decomposition and leading to lower NH_3 yields upon reaction with H_2 [20,26]. In the present study, similar result to that obtained for the iron containing system was obtained upon cobalt addition and only limited amount of ammonia was produced after 6 h of reaction ca.273 μmol/g.

3.2.3. Reactivity of A-Mn-N (A= K, Li)

The effect of alkali metal on Mn_3N_2 lattice nitrogen reactivity was studied for Li and K containing materials A-Mn-N (Table 2, Fig. 10). Upon potassium addition, ammonia synthesis was strongly suppressed and only a very limited amount was produced during the first two hours of reaction. In spite of potassium being reported as an efficient promoter for iron [27] and rhenium [28] based catalysts no enhancement on the reactivity of Mn_3N_2 was observed. In contrast, the nitrogen transfer properties were considerably enhanced when lithium was used as co-metal, ~1306 ± 44 μmol NH_3/g is generated during the first 5 h of reaction and a total of ~1571 ± 53 μmol NH_3/g was generated after 15 h. The quantity of ammonia produced at the end of reaction corresponds to the reaction of 18% of the total available lattice nitrogen compared initially to 3.1% in Mn_3N_2. Furthermore, post-reaction CHN analysis confirmed the reduction of N- content in the Li-Mn-N system to 0.5 wt%.

The temperature dependence of nitrogen reactivity was assessed by conducting the ammonia synthesis reaction at different temperatures (Fig. 11, Table 3). At low temperature, T = 300 °C, the material demonstrated high nitrogen reactivity as evidenced by the significant amount of ammonia produced ~1306 ± 44 mol NH_3/g which corresponded to ~15.8% of the total available lattice nitrogen. Conducting ammonia synthesis reaction at higher tem-

Table 3
Summary of nitrogen reactivity of lithium manganese nitride related materials after reaction with 60 ml min^{-1} of 1:3 N_2:H_2.

	Temperature reaction/°C	Total N content/μmol/g of material	NH_3 produced/μmol after 5h	% lattice N converted to NH_3
Li-Mn-N	300	8644 ± 17	1400 ± 48	16.2
	400	8644 ± 17	1306 ± 44	15.8
	500	8644 ± 17	2072 ± 70	24.0

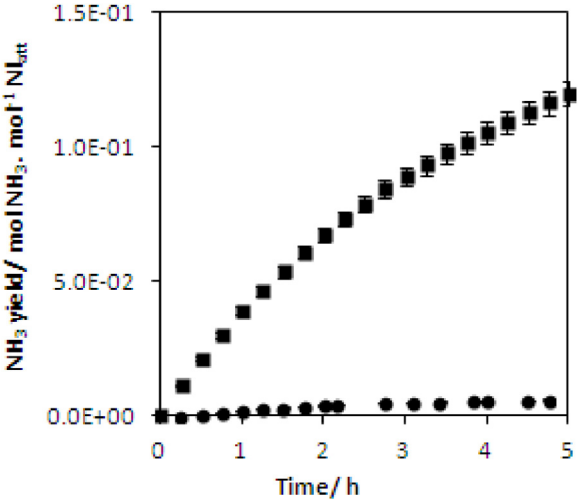

Fig. 10. Ammonia yield of A-Mn-N with 60 ml min^{-1} of 1:3 N_2: H_2 at 400 °C: (●) K-Mn-N, (■) Li-Mn-N. Error propagation within a 95% confidence interval.

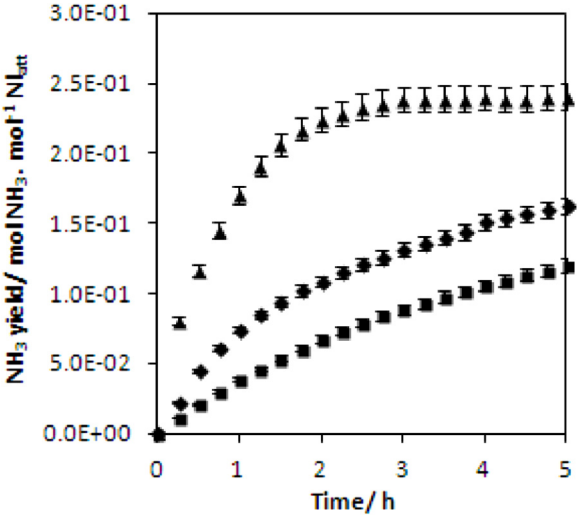

Fig. 11. Ammonia yield of Li-Mn-N, with 60 ml min^{-1} of 1:3 N_2: H_2 as a function of temperature: (■) 300 °C, (♦) 400 °C and (▲) 500 °C. Error propagation within a 95% confidence interval.

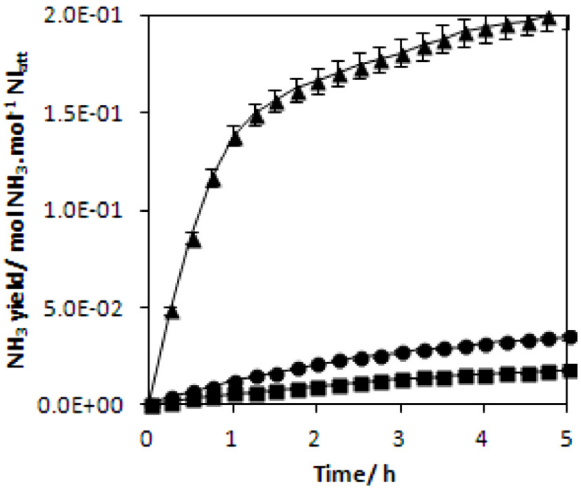

Fig. 12. Regenerability of Li-Mn-N: (▲) first cycle, (●) second cycle and (■) third cycle. Reduction step conducted with 60 ml min^{-1} of 1:3 Ar: H_2 at 400 °C. The nitridation step was conducted with 60 ml min^{-1} flow of N_2 at 800 °C. Error propagation within a 95% confidence interval.

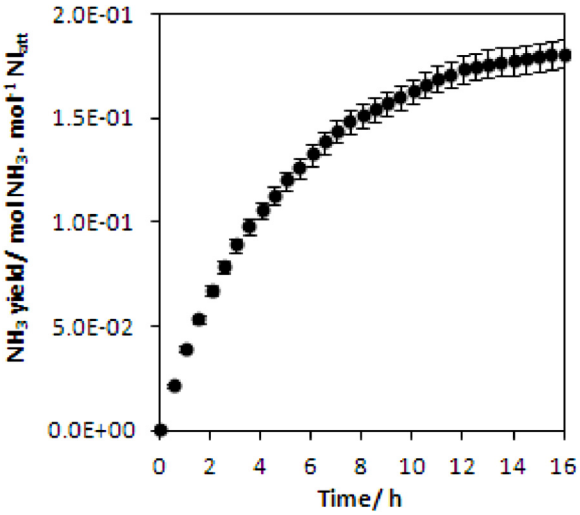

Fig. 13. Ammonia yield of Li-Mn-N with 60 ml min^{-1} of 1:3 N_2: H_2 at 400 °C for 16 h. Error propagation within a 95% confidence interval.

perature, T = 500 °C, resulted in considerable enhancement of the amount of ammonia generated to ~2072 ± 70 μmol NH_3/g which corresponded to the consumption of ~24% of the total available lattice nitrogen. However, most of the ammonia was generated during the first two hours of reaction and only a small amount of ammonia was produced thereafter.

3.2.4. Nitrogen charge-discharge properties of Li-Mn-N

The regenerability of the Li-Mn-N system was examined by alternating dintridation (N- discharge) and nitridation (N- charge) cycles under different conditions (Fig. 12). The reduction step was conducted using 60 ml min^{-1} flow of a 1:3 Ar: H_2 at 400 °C while the nitridation step was conducted using 60 ml min^{-1} flow of N_2 at 800 °C. Fig. 13 shows the reactivity of the Li-Mn-N system over three cycles. During the first reduction cycle, high reactivity was observed and ~1738 ± 59 NH_3 μmol/g was generated after 5 h of reaction. However, when subject to a regeneration step under a flow of N_2 at 800 °C for 5 h, Li-Mn-N presented limited reactivity and only a small amount of ammonia 304 ± 10 μmol NH_3/g and 159 ± 5 μmol NH_3/g was generated after the second and the third cycles respectively. Despite efforts to close the thermochemical ammonia production cycle by regenerating the material using N_2 at high temperature, elemental analysis showed consumption of lattice nitrogen after the denitriding – nitriding cycles. Prolonging the regeneration step

to 12 h did not affect the regenerability of Li-Mn-N system and no further regain of reactivity was observed during the third cycle of reduction. A decrease of 24% of lithium concentration with respect to the initial concentration of Li in Li-Mn-N system was observed after the denitridation-nitridation cycles.

3.3. Nitrogen bulk transfer properties on manganese related material

The dependence of nitrogen transfer properties upon chemical composition and temperature was evaluated using ammonia synthesis as a model reaction. In view of the reactivity results and post reaction analysis, ammonia synthesis proceeds through a process akin to the Mars – van Krevelen mechanism involving lattice nitrogen reaction. Thus, the amount of ammonia produced during reactivity test can be linked to lattice nitrogen transfer properties of manganese related materials as: $A\text{-}Mn\text{-}N_x + 3/2\delta H_2 \rightarrow A\text{-}Mn\text{-}N_{x-\delta} + \delta NH_3$

In Mn_3N_2, lattice nitrogen reactivity was evidenced by the ammonia synthesis reaction. Unfortunately only a very limited fraction was reactive towards dihydrogen and most of the lattice nitrogen was lost as N_2. Adding a co-metal to manganese nitride provided a route to alter lattice N- reactivity. However, the addition of cobalt, iron or potassium resulted only in enhancing lattice nitrogen depletion as N_2. However, adding low levels of lithium improved considerably the reactivity of manganese lattice nitrogen towards hydrogen at low temperature. Since lattice nitrogen reactivity has been evidenced in all the A-Mn-N systems, the higher reactivity of Li-Mn-N possibly could be attributed to dihydrogen activation by lithium. The role of lithium in enhancing the performance of materials is an area currently undergoing further investigation. In this context, it is interesting to draw intention to a similar positive effect of LiH addition to Mn_2N activity for ammonia synthesis as recently reported by Chen and co-workers [23]. The authors presented a "two-active centre catalyst", where lithium's role was to remove N_{ad} from the surface and activate the hydrogenation step whereas the Mn(N) surface activates N_2 in a continuous manner. LiH-Mn, Mn to LiH molar ratio of about 1:5, was presented as highly active catalyst for ammonia synthesis reaction and showed stability during 10 h of reaction. In our case, Li-Mn-N (Mn to Li molar ratio of about 1:10) behaved more as a nitrogen transfer reagent rather than a catalyst with ~16% of its lattice nitrogen being reactive towards dihydrogen to yield ammonia at temperatures as low as 300 °C. The reactivity of in the Li-Mn-N system was maintained up to complete depletion of lattice nitrogen which was only achieved after 16 h of reaction (Fig. 13). As ammonia production proceeds in the Li-Mn-N system through a pathway akin to the Mars van Krevelen mechanism, it is possible that the rate-determining step for NH_3 synthesis during the denitridation cycle is nitrogen transfer from the lattice to the surface which might explain the higher rates reported on Li-Mn-N systems when compared to classical formulations. However, the results of denitridation-nitridation cycles suggest that the limiting step of the overall process is associated with regeneration of the looping materials with N_2. In order to further explore this aspect, the role of dopants in the activation of nitrogen and hydrogen during the different cycles is currently under investigation by means of isotopic exchange reactions.

Another, indirect, aspect of our studies is that they illustrate the necessity for prolonged activation testing and post-reaction N-analysis when applying nitrides to ammonia synthesis. Initial cursory information may suggest that systems are catalytic when, in fact, they may not and may be functioning as reagents.

4. Conclusion

In this work, manganese related materials A-Mn-N, A = Fe, Co, K, Li systems, were synthesised by a soft chemistry synthesis technique using $NaNH_2$ as a source of reactive nitrogen. The impact of chemical composition upon lattice nitrogen reactivity was studied. Although, lattice nitrogen mobility has been evidenced in all the A-Mn-N systems, only Li-Mn-N presented high nitrogen reactivity towards hydrogen which may be attributed to dihydrogen activation by lithium. Reactivity tests and post-reaction analysis confirmed that A-Mn-N systems are better described as reagents than catalytic system.

Acknowledgements

We are grateful to M. G. Reddy for very kindly conducting the nitrogen elemental analyses. We thank the Engineering and Physical Sciences Research Council for the provision of funding through grants EP/L02537X/1 and EP/L026317/1.

Appendix A. Supplementary data

Supplementary data associated with this article can be found, in the online version, at http://dx.doi.org/10.1016/j.apcatb.2017.04.073.

References

[1] S. Enthaler, ChemSusChem 3 (2010) 1024–1029.
[2] D.M. Roundhill, Chem. Rev. 92 (1992) 1–27.
[3] P.B. Cranwell, M. O'Brien, D.L. Browne, P. Koos, A. Polyzos, M. Pena-Lopez, S.V. Ley, Org. Biomol. Chem. 10 (2012) 5774–5779.
[4] V. Amarnath, D.C. Anthony, K. Amarnath, W.M. Valentine, L.A. Wetterau, D.G. Graham, J. Org. Chem. 56 (1991) 6924–6931.
[5] A. Mittasch, Adv. Catal. Relat. Subj. II (1950) 81–104.
[6] L. Andrussow, Angewandte Chemie 48 (1935) 593–595.
[7] O. Wilhelm, Improvements in the Manufacture of Nitric Acid and Nitrogen Oxides, 1902.
[8] Y. Tanabe, Y. Nishibayashi, Coord. Chem. Rev. 257 (2013) 2551–2564.
[9] A.M. Alexander, J.S.J. Hargreaves, C. Mitchell, Top. Catal. 56 (2013) 1963–1969.
[10] A.M. Alexander, J.S.J. Hargreaves, C. Mitchell, Top. Catal. 55 (2012) 1046–1053.
[11] S.M. Hunter, D.H. Gregory, J.S.J. Hargreaves, M. Richard, D. Duprez, N. Bion, ACS Catal. 3 (2013) 1719–1725.
[12] G.E. Veitch, K.L. Bridgwood, S.V. Ley, Org. Lett. 10 (2008) 3623–3625.
[13] G.E. Veitch, K.L. Bridgwood, K. Rands-Trevor, S.V. Ley, Synlett (2008) 2597–2600.
[14] C.D. Zeinalipour-Yazdi, J.S.J. Hargreaves, C.R.A. Catlow, J. Phys. Chem. C 119 (2015) 28368–28376.
[15] D. Zhu, L. Zhang, R.E. Ruther, R.J. Hamers, Nat. Mater. 12 (2013) 836–841.
[16] J.R. Christianson, D. Zhu, R.J. Hamers, J.R. Schmidt, J. Phys. Chem. B 118 (2014) 195–203.
[17] J. Soria, J.C. Conesa, V. Augugliaro, L. Palmisano, M. Schiavello, A. Sclafani, J. Phys. Chem. 95 (1991) 274–282.
[18] Y. Abghoui, A.L. Garden, J.G. Howalt, T. Vegge, E. Skúlason, ACS Catal. 6 (2016) 635–646.
[19] S. Laassiri, C.D. Zeinalipour-Yazdi, C.R.A. Catlow, J.S.J. Hargreaves, Catal. Today 286 (2017) 147–154.
[20] R. Michalsky, A.M. Avram, B.A. Peterson, P.H. Pfromm, A.A. Peterson, Chem. Sci. 6 (2015) 3965–3974.
[21] M.D. Lyutaya, A.B. Goncharuk, Soviet Powder Metall. Metal Ceram. 16 (1977) 208–212.
[22] R. Yu, X. Chong, Y. Jiang, R. Zhou, W. Yuan, J. Feng, RSC Adv. 5 (2015) 1620–1627.
[23] P. Wang, F. Chang, W. Gao, J. Guo, G. Wu, T. He, P. Chen, Nat. Chem. 9 (2017) 64–70.
[24] A. Miura, T. Takei, N. Kumada, Inorg. Chem. 52 (2013) 11787–11791.
[25] C.S. Johnson, N. Li, C. Lefief, J.T. Vaughey, M.M. Thackeray, Chem. Mater. 20 (2008) 6095–6106.
[26] R. Michalsky, P.H. Pfromm, A. Steinfeld, Interface Focus 5 (2015) (2014.0084).
[27] G. Ertl, M. Weiss, S.B. Lee, Chem. Phys. Lett. 60 (1979) 391–394.
[28] C. Liang, Z. Wei, Q. Xin, C. Li, Appl. Catal. A: Gen. 208 (2001) 193–201.